

Changing Computing Paradigms Towards Power Efficiency

Pavel Klavík¹, A. Cristiano I. Malossi², Costas Bekas²,
Alessandro Curioni²

¹Charles University in Prague,
Faculty of Mathematics and Physics,
Computer Science Institute,
Malostranské nám. 25,
118 00 Prague, Czech Republic
e-mail: klavik@iuuk.mff.cuni.cz

²IBM Research - Zurich,
Säumerstrasse 4,
CH-8803, Rüschlikon,
Switzerland
e-mail: {acm,bek,cur}@zurich.ibm.com

Power awareness is fast becoming immensely important in computing, ranging from the traditional High Performance Computing applications, to the new generation of data centric workloads.

In this work we describe our efforts towards a power efficient computing paradigm that combines low precision and high precision arithmetic. We showcase our ideas for the widely used kernel of solving systems of linear equations that finds numerous applications in scientific and engineering disciplines as well as in large scale data analytics, statistics and machine learning.

Towards this goal we developed tools for the seamless power profiling of applications at a fine grain level. In addition, we verify here previous work on post FLOPS/Watt metrics and show that these can shed much more light in the power/energy profile of important applications.

Subject Areas: Computer Science; High Performance Computing; Numerical Analysis

Keywords: Energy-aware Computing; Power Consumption; Performance Metrics; Cholesky Method; Conjugate Gradient Method

Published in: Philosophical Transactions of the Royal Society A: Physical, Mathematical and Engineering Sciences 372(2018), 2014, in the Theme Issue 'Stochastic modelling and energy-efficient computing for weather and climate prediction'.

DOI: 10.1098/rsta.2013.0278,

URL: <http://rsta.royalsocietypublishing.org/content/372/2018/20130278>.

1. Introduction

Since the 1970's the High Performance Computing community, including industry and academia, have tremendously benefited from the existence of a single, simple, and easy to deploy benchmark: the LINPACK benchmark [6]. Its original target was the solution of a dense linear system of 1000 equations in the minimum time, thus generating a ranking of the most powerful supercomputers based on the measured number of floating point operations per unit of time (FLOPS). As supercomputers became increasingly more potent, the LINPACK benchmark evolved allowing to scale the problem size, while keeping the same goal. Indeed, while early machines achieved Mega-FLOPS, today's most powerful supercomputers reach Peta-FLOPS, which constitutes an astonishing increase of nine orders of magnitude in less than 35 years.

Since 1993 a list of the most powerful supercomputers has been kept and updated bi-annually in June and November: this is the famous TOP500 list¹. It graphically portrays this exponential increase in performance, that is attributed mostly to Moore's law, which in turn has been widely (and vaguely) interpreted as an exponential performance improvement in CMOS technology. However, during the last decade, the core technology has dramatically changed. Voltage and thus frequency scaling has stopped, pointing out the true nature of Moore's law, which essentially predicted our technological capacity to exponentially increase the number of logical gates on a chip. To continue the exponential overall improvements, technologists have turned into multi-core chips and parallelism at all scales. However, this new trend has led to a series of new issues and questions, which nowadays represent the most critical aspects in the development of future architectures and software. These questions are mainly: (i) How to program such complex machines? (ii) How to cope with the very fast increase in power requirements? In this work we concentrate on the latter one, although we believe that programmability and energy efficiency will ultimately prove to be closely connected.

In [2], the authors have shown that very important power savings can be achieved by a careful combination of different precision levels for floating point arithmetic. Those observations led to introduction of new energy-aware performance metrics. This was motivated by the fact that the traditional energy-aware performance metrics (derived from the classic FLOPS performance metric) have serious shortcomings and can potentially draw a picture that is far from reality. For instance, the widespread FLOPS/Watt metric, which is used to rank supercomputers in the Green500 list², might still promote power hungry algorithms instead of other more energy efficient techniques. In contrast, by using metrics based on both time to solution and energy, as proposed in [2], it is possible to get a much more realistic picture, which can drive and help the design of future energy efficient machines and algorithms. At the same time, we also need to abandon the (convenient and simple) LINPACK benchmark and make use of a relatively small selected set of benchmarks, characterized by widely different features and thus representative of the majority of the current applications [1,12].

¹<http://top500.org>

²<http://green500.org>

The reasoning for the mixed precision computing paradigm and the associated energy-aware performance metrics in [2] is based on a model of power consumption for the various subsystems of a computing platform, such as the floating point unit, the interconnect, and the memory; this model is an extrapolation of future exascale machines [15]. At the same time, it is widely acknowledged that actual on-line measurements can be complicated and require external circuits that cast noise in the measurements. Recent advances in chip technology however have allowed the on chip measurement of instantaneous power consumption by means of integrated sensors [5, 7,13,16]. In this work we advance the initial contribution in [2] and describe a fully automated, on-line, minimally invasive system for measuring power performance. Our tool follows a similar philosophy to other tools such as PowerPack 3.0³ package [8], however we have put here emphasis on minimizing measurement noise and fine granularity. Our system allows users to easily instrument their code, as well as to directly distinguish and separately measure power performance of various code segments. The tool is completed by a carefully designed graphical interface, which provides real-time, easy-to-read informative plots and diagrams.

The target platform of our analysis is the IBM POWER7 processor, that offers a wide variety of on-chip sensors. On this machine we perform a series of analysis that confirms and extends findings and theories devised in [2] on an IBM Blue Gene/P system. More importantly, we outline a general energy-aware framework for solving linear systems, that is based on a careful combination of mixed-precision arithmetics. In addition, we take a further step and show that our framework allows the use of inaccurate data, as well as inaccurate computations. That is particularly crucial as data movement is expected to completely dominate running time and power consumption in future systems.

This work is organized as follows. In Section 2 we describe our framework for on-line, on chip power consumption measurements. In Section 3 we describe the inexact computing/data framework for solving systems of linear equations. Then, in Section 4 we present our experimental results applied to covariance matrices from applications in data-analytics. We conclude with remarks in Section 5.

2. On-line – on chip power measurement

In this section we describe the framework that we set up to perform power measurements. Our system consists of an IBM blade server PS702⁴ [17], with two IBM POWER7 chips (octa core, 3.00 GHz CPU and 4 MB L3-cache each) and 64 GB of system memory. Each POWER7 chip has several embedded thermal sensors which measure the temperature of the different components. Data from sensors are transferred to a separate service processor that is embedded in the POWER7 server. The service processor is running a firmware called AME Driver which in turn calculates power from the thermal sensors as described in [7,13,16]. We remark that it is crucial that power readings are calculated on the service processor, so they do not add background noise

³<http://scapecs.vt.edu/software/powerpack-3-0/>

⁴<http://www-03.ibm.com/systems/bladecenter/hardware/servers/ps700series/specs.html>

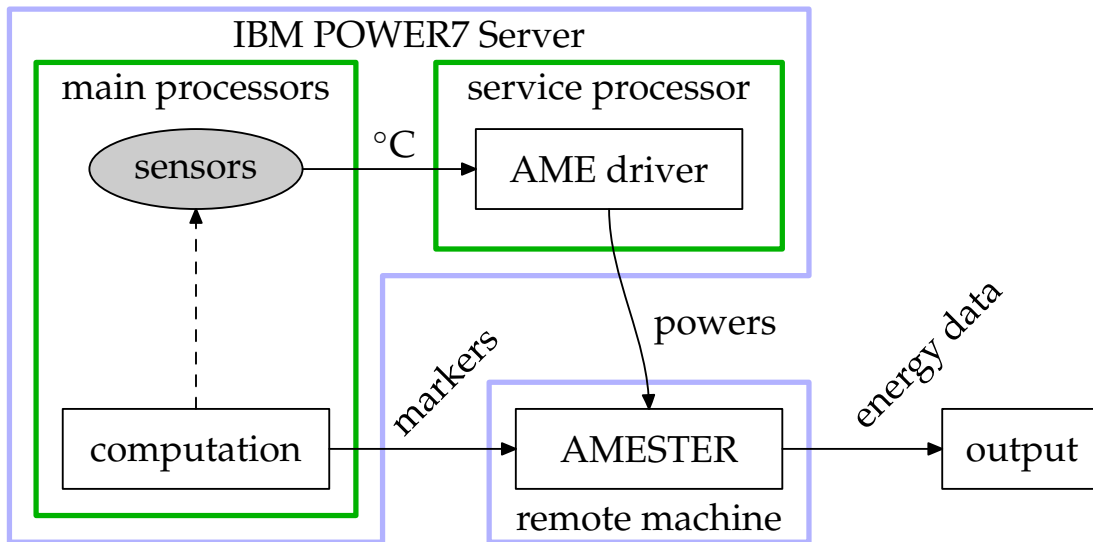


Figure 1: Schematic description of the experimental framework for power measurements.

to the actual user computation; in this regard the POWER7 server is an ideal platform to perform power measurements. Finally, on a remote machine we run a software named AMESTER (Automated Measurement of Systems for Energy and Temperature Reporting). This is an experimental application developed by IBM, which periodically retrieves power measures from the service processor of the POWER7 server and collects them into a file (for more details see [13,16]). A graphical description of the power measurement framework is depicted in Figure 1.

To ease the instrumentation of the code, we have developed a library that provides a black-box interface between AMESTER and the running application. This layer uses TCP/IP sockets hidden behind a series of simple calls. Issues of TCP/IP latency and resolution of instrumentation are directly resolvable since the AME Driver allows for a store/trace forward mode, where a bunch of power data is measured and collected such that it can be subsequently read remotely. Thus instrumentation permits to setup and run AMESTER, and then mark power data during computation; using this framework we can map measured data to different parts of the code and get a clear picture of the specific power consumption for each analyzed kernel in our application. The resolution of power is less than 1 W while the sampling frequency is approximately 1 kHz (i.e., up to 1000 samples per second). The error of the power measurements is stated to be lower than 2% [7,14,17].

An example of power analysis is illustrated in Figure 2, where we plot measurements from five power sensors during an idle state of the machine. From top to bottom these are: total power of the system, power of each of the two processors, and power of each of the corresponding memory banks. Note that the total power of the system includes additional sources of power consumption, such as disks and fans, which in the idle state consume approximately 30 W. These values are averaged in time in Table 1, providing us the lower bound limit of power consumption of the PS702 blade server. In the examples

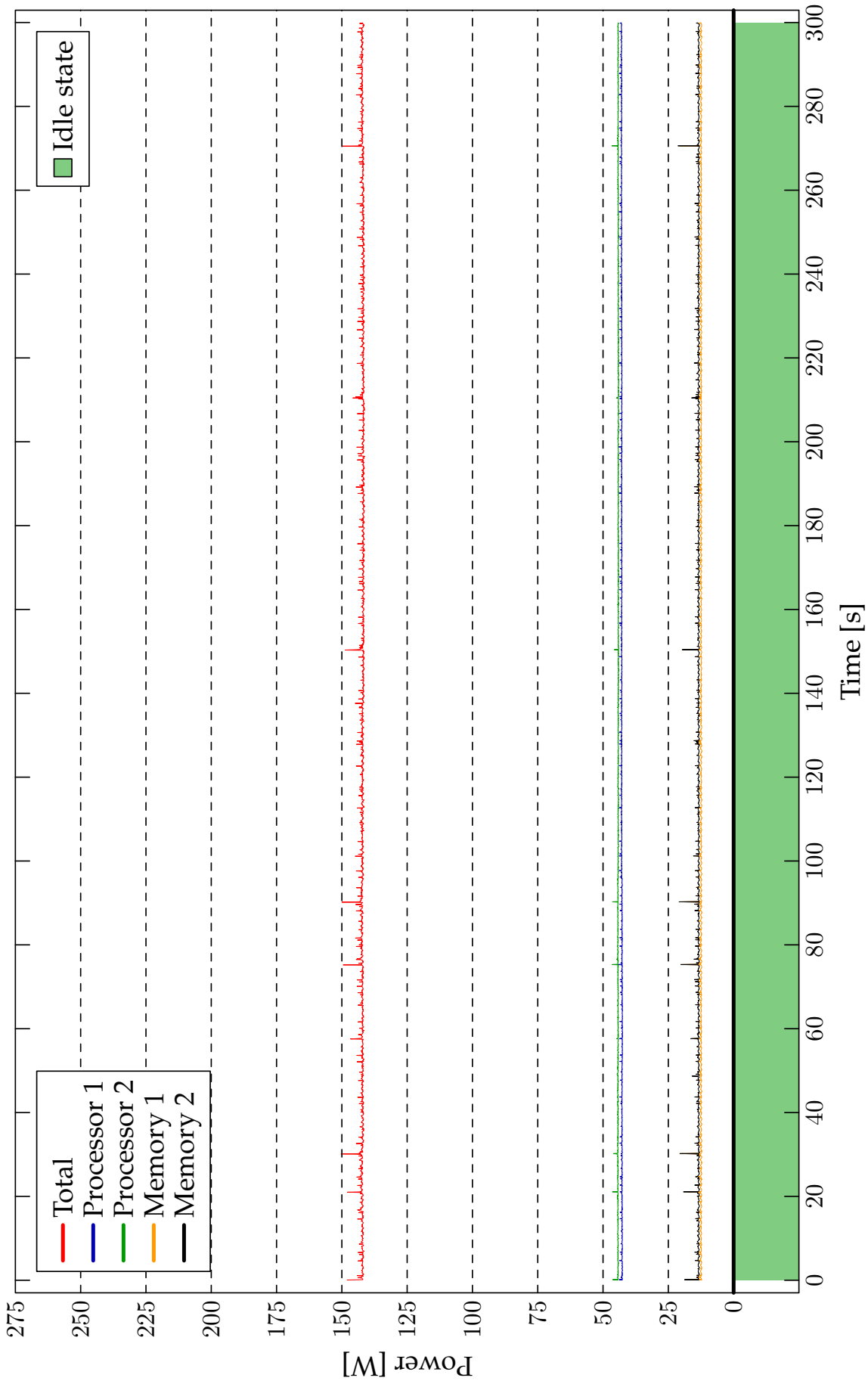


Figure 2: Power of chips and memories on the IBM blade server PS702 during an idle state.

Table 1: Average power (over 300 seconds) of chips and memories on the IBM blade server PS702 during an idle state.

Sensor	Average power [W]	Standard error [W]
Total	142.1	0.6
Processor 1	42.8	0.2
Processor 2	44.2	0.2
Memory 1	12.5	0.4
Memory 2	13.4	0.4

presented in the forthcoming sections, we will observe that chip power can reach up to 80 W, while memory power can get up to 40 W. Total power is thus always between 140 W and 200 W.

3. Inexact solving of dense linear systems

Let us focus on the solution of a dense system of n linear equations in the form

$$A\mathbf{x} = \mathbf{b}, \quad (3.1)$$

where $A \in \mathbb{R}^{n \times n}$ is a symmetric and positive definite matrix, $\mathbf{x} \in \mathbb{R}^n$ the solution vector, and $\mathbf{b} \in \mathbb{R}^n$ the right-hand side. This problem can be generalized to the case of m right-hand sides $\mathbf{b}_1, \dots, \mathbf{b}_m$ such that we can write

$$AX = B, \quad (3.2)$$

where $B = [\mathbf{b}_1, \mathbf{b}_2, \dots, \mathbf{b}_m] \in \mathbb{R}^{n \times m}$ and $X = [\mathbf{x}_1, \mathbf{x}_2, \dots, \mathbf{x}_m] \in \mathbb{R}^{n \times m}$ are two rectangular matrices containing all the right-hand sides and solution vectors, respectively.

The target of our analysis is the solution of large size covariance matrix problems, which are crucial for uncertainty quantification and applications in data-analytics (see, e.g., [4] and references therein). With this aim, in the following we describe two iterative refinement procedures derived from the Cholesky and the conjugate gradient (CG) methods for the solution of this class of problems.

(a) Cholesky with iterative refinement

The Cholesky decomposition $A = R^T R$ (see, e.g., [9]) offers a cache friendly and high performance approach for the solution of problems (3.1) and (3.2). The overall complexity of the decomposition is $1/3 n^3 + \mathcal{O}(n^2)$. Once it is done, the solution of the problem can be computed very fast, even for multiple right-hand sides:

$$X = R^{-1} R^{-T} B, \quad (3.3)$$

Algorithm I : Cholesky method with iterative refinement for one right-hand side.

- | | |
|--|------------------|
| 1: Compute Cholesky decomposition $A \approx \tilde{R}^T \tilde{R}$. | [Low precision] |
| 2: Generate approximate solution $\mathbf{x} = \tilde{R}^{-1} \tilde{R}^{-T} \mathbf{b}$. | [Low precision] |
| 3: Compute residual $\mathbf{r} = \mathbf{b} - A\mathbf{x}$. | [High precision] |
| 4: while $\ \mathbf{r}\ _2 \geq \text{tolerance}$ | |
| 5: Compute error components $\mathbf{z} = \tilde{R}^{-1} \tilde{R}^{-T} \mathbf{r}$. | [Low precision] |
| 6: Update solution $\mathbf{x} = \mathbf{x} + \mathbf{z}$. | [High precision] |
| 7: Compute residual $\mathbf{r} = \mathbf{b} - A\mathbf{x}$. | [High precision] |
| 8: end | |
-

where we remark that R is an upper-triangular matrix; consequently the cost of (3.3) is $\mathcal{O}(n^2)$ per right-hand side vector, thus in general negligible.

In [3,4] (see also references therein), it has been shown that to cope with the formidable cubic cost of the Cholesky decomposition, mixed precision iterative refinement can be employed. For instance, let us consider the procedure described in Algorithm I for the case of a single right-hand side, where we use the “ \sim ” symbol to denote matrices or vectors stored in low precision. On modern multicore chips with accelerators, the computation of the Cholesky decomposition at the very first step can be speedup by using IEEE single precision arithmetics. The resulting inexact-decomposition is then used also at line 5 of Algorithm I for each iteration till convergence.

Observe however that the complexity of the overall scheme remains $\mathcal{O}(n^3)$, due to the matrix factorization. Therefore, even with significant single precision acceleration, time-to-solution increases cubically with the matrix size and dominates the computation in case of large problems. A second important remark concerns the very nature of dense matrix factorizations, such as the Cholesky decomposition. These are rich in BLAS-3, cache friendly linear algebra primitives, a property that has been the focus of attention for optimizing system performance. It reflects that codes like the Cholesky decomposition tend to make full use of the computational resources of the system, stressing its components to their limits.

As an example, Figure 3 shows power measurement for solving a linear system with 32 right-hand sides using the Cholesky decomposition and mixed precision iterative refinement. It is evident that the majority of time and energy is spent for the Cholesky decomposition. In addition, note that power consumptions peaks around 200 W, due to the BLAS-3 primitives that ensure high sustained performance in the arithmetic computations.

The burning question thus, is whether it is possible to fundamentally reduce the computational cost. Iterative refinement theory predicts that the only requirement for the process to converge is that the solver used for the inner step at line 5 of Algorithm I is not too ill-conditioned [11]. In particular, the following conditions need to be satisfied:

$$(A + \Delta A)\mathbf{z} = \mathbf{r} \quad \text{and} \quad \|A^{-1} \Delta A\|_{\infty} < 1, \quad (3.4)$$

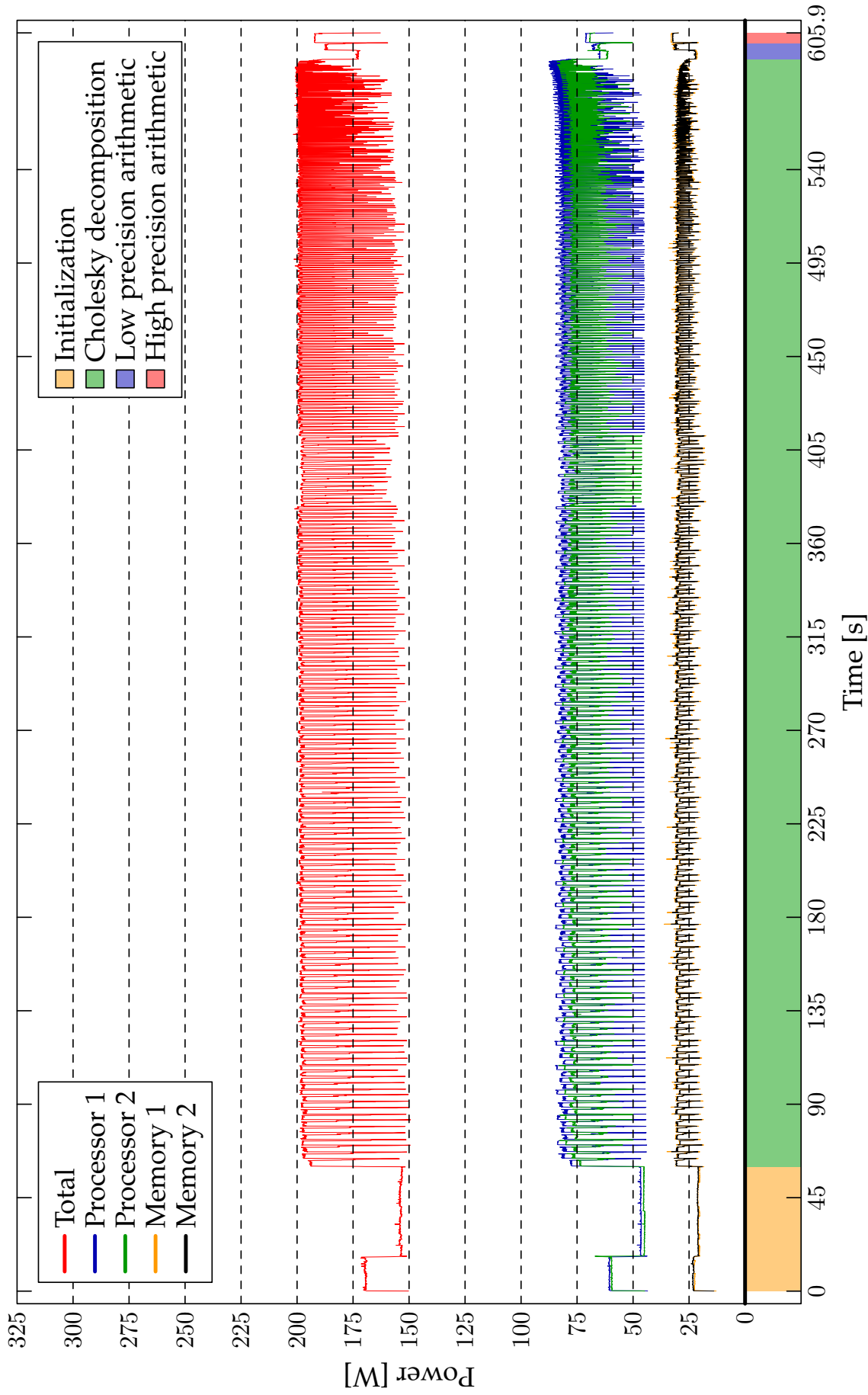


Figure 3: Power diagram on IBM PS702 Blade Server during the solution of a dense linear system with 32 right-hand sides, employing the Cholesky based approach with iterative refinement. In the timeline, each computational phase is displayed with a different color.

where ΔA is a given perturbation of the matrix coefficients. In the iterative refinement setting, this perturbation corresponds to the error introduced by storing the matrix (or its factorization), in low precision. Bound (3.4) implies that if the problem is not too ill-conditioned, then the iterative scheme would still be able to converge with the desired high precision, even if the accuracy of the internal solver is quite low.

To see this, consider the results of [3,4] depicted in Figure 4: there we plot the number of iterations to solve a dense linear system up to working precision (in our case, IEEE double precision), by using a perturbed Cholesky algorithm. In particular, the factor R (computed in double precision) is perturbed with a range of upper-triangular matrices E , whose norm is such that $\|R + E\|_2 / \|R\|_2 \leq 10^\gamma$, with $\gamma \in \{-1, -3.25, -5.5, -7.75, -10\}$. This experiment evidently demonstrates that even in presence of large perturbations, e.g., $\gamma = -1$, the method is still able to converge. Moreover, even if the number of iterations increases, each one of them costs $\mathcal{O}(n^2)$ which is generally several orders of magnitude less than the Cholesky decomposition.

This example shows clearly that the accuracy of the employed solver can be lowered without compromising the robustness of the numerical scheme. In fact, the very nature of the solver we choose is quite irrelevant, with the only crucial property being that of bound (3.4).

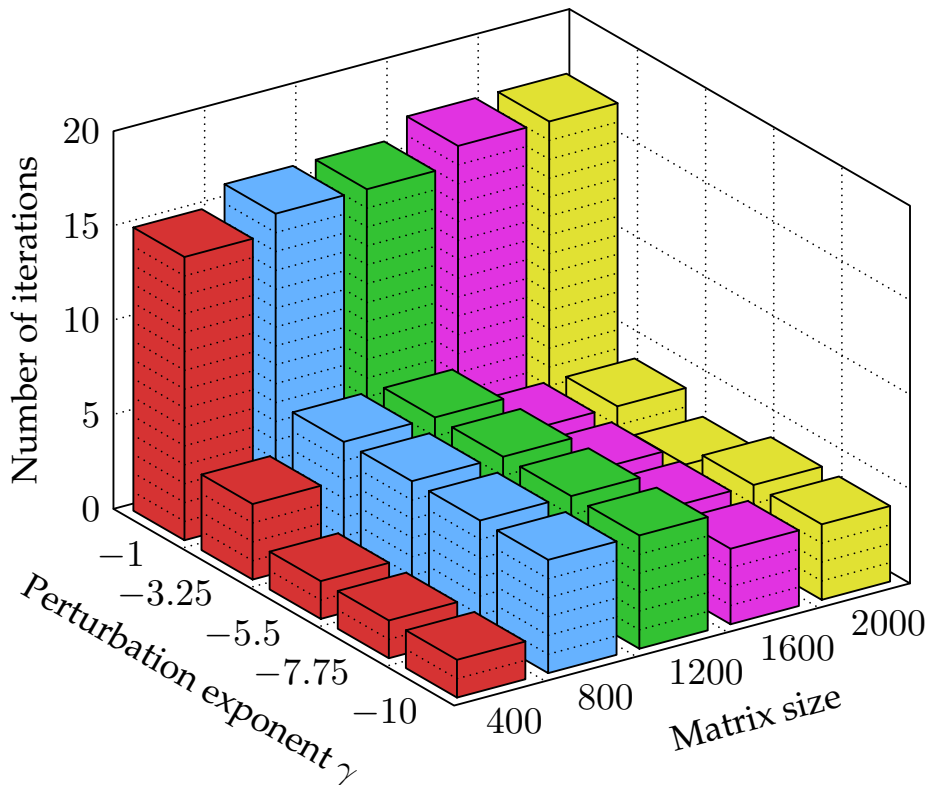


Figure 4: The number of iterations to solution of a perturbed Cholesky algorithm, for a range of matrix sizes and perturbation exponents.

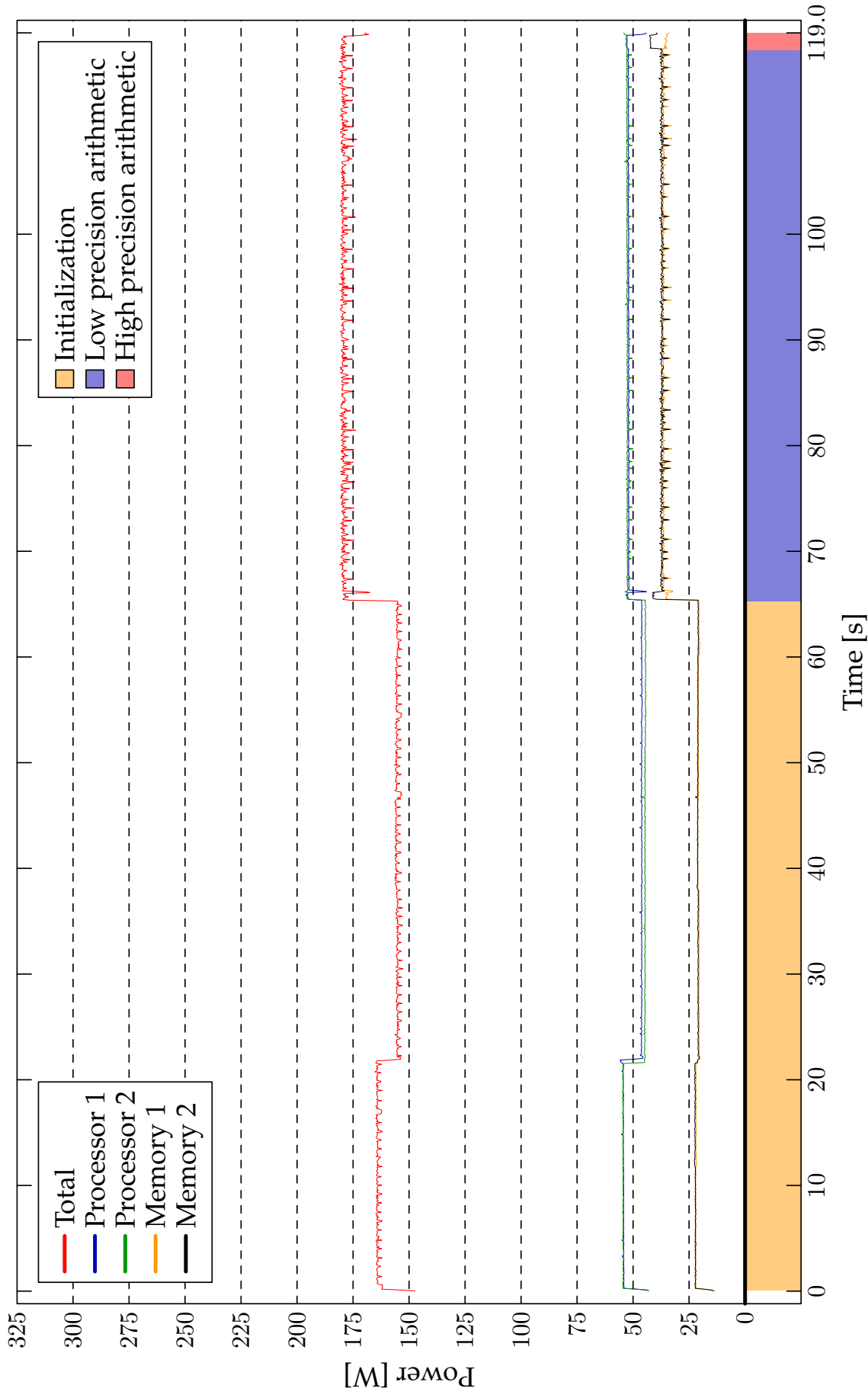


Figure 5: Power diagrams on IBM PS702 Blade Server during the solution of a dense linear system with 1 right-hand side using the conjugate gradient algorithm with iterative refinement. In the timeline, each computational phase is displayed with a different color.

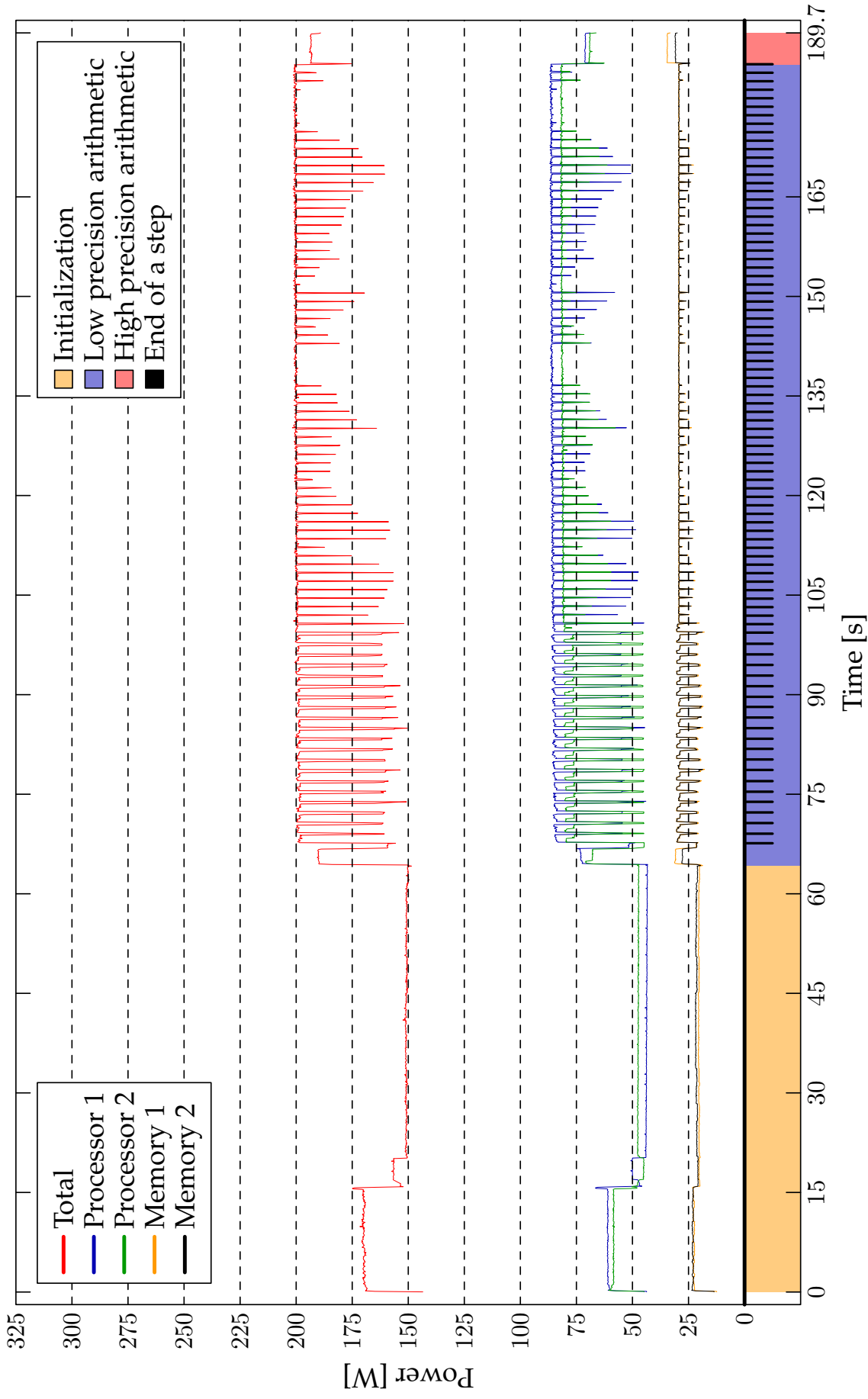


Figure 6: Same as Figure 5 but for 32 right-hand sides. In the timeline, each computational phase is displayed with a different color, while the end of each step is marked by a black line.

Algorithm II : Conjugate gradient method with iterative refinement for one right-hand side.

- 1: Set initial solution $\mathbf{x} = \mathbf{x}_0$.
 - 2: Compute residual $\mathbf{r} = \mathbf{b} - A\mathbf{x}$. [High precision]
 - 3: Set initial direction $\mathbf{p} = \mathbf{r}$.
 - 4: **while** $\|\mathbf{r}\|_2 \geq \text{tolerance}$
 - 5: Compute matrix-vector multiplication $\mathbf{z} = \tilde{A}\mathbf{p}$. [Low precision]
 - 6: Compute $\rho = \mathbf{r}^\top \mathbf{r}$ and $\alpha = \rho / (\mathbf{p}^\top \mathbf{z})$. [High precision]
 - 7: Update solution $\mathbf{x} = \mathbf{x} + \alpha\mathbf{p}$. [High precision]
 - 8: Update residual $\mathbf{r} = \mathbf{r} - \alpha\mathbf{z}$. [High precision]
 - 9: Compute $\beta = (\mathbf{r}^\top \mathbf{z}) / \rho$ and update direction $\mathbf{p} = \mathbf{r} + \beta\mathbf{p}$. [High precision]
 - 10: **end**
-

(b) Conjugate gradient with iterative refinement

In [4] (see also [3]) the conjugate gradient method with iterative refinement (see Algorithm II) is proposed as a possible energy-efficient replacement of the Cholesky based approach. Particularly, it is shown that the overall computational cost can be reduced down to quadratic levels from the original cubic cost of dense solvers.

Figure 5 illustrates power measurements for this approach, solving the same problem as in the Cholesky based version, but with one right-hand side. First of all, we observe that time-to-solution is strongly reduced as compared to the Cholesky based method. Indeed, there is no initial factorization phase any longer that dominates the run time. A second observation regards the peak power consumption which, with respect to the idle state, is about 50% less than the peak power observed for the Cholesky case in Figure 3.

When increasing the number of right-hand sides from 1 to 32, as shown in Figure 6, the major internal kernel of the CG based algorithm becomes the matrix-matrix multiplication, and thus peak power characteristics resemble those of the Cholesky based approach. The sudden decreases in power are due to executing vector operations (BLAS-2), which do not stress the system as much as BLAS-3 based computations. We also notice that the first few steps take longer time before the machine moves the data in right caches. As a consequence, in the case of the multiple right-hand sides, it is by far the decreased time-to-solution that drives the decrease in total energy of the CG based method with respect to the Cholesky one.

4. Iterative refinement on approximate covariance matrices

Bound (3.4) offers a second reading: we can cast the error not to the employed solver, but to the data. Indeed, this is a statement akin to the classical backward stability. In other words, we can use an *exact* solver that works on *inexact* data, as shown in the example of the perturbed Cholesky factor discussed in Section 3.

A possible strategy to take advantage of this approach, is to approximate the system matrix by following the pattern in its structure. For instance, in several applications matrices exhibit a progressive decay of their elements away from the main diagonal. In those cases, a reduced banded version of the matrix (with just a few diagonals) can be used, in place of the complete one. Observe that the resulting complexity of the inner solver is drastically reduced, as well as data movement requirements, which are lowered by almost one order of magnitude. We call this solver *banded CG* and its power diagrams are in Figure 7 and Figure 8.

In general, we can opt for sampled versions of the matrices involved for the inner solver. To this end we can borrow approaches developed in the literature of randomized linear algebra (see, e.g., [10] and references therein). The main idea is that matrix A is replaced by $\tilde{A} = PAP^T$ where P is a suitably chosen fat sketching matrix $P \in \mathbb{R}^{k \times n}$ where $k \ll n$.

In the following, we showcase the validity of our arguments with a set of numerical experiments using model covariance matrices with controlled degree of decay d away from the main diagonal:

$$A(i, j) = \begin{cases} \frac{1}{|i - j|^d} & i \neq j, \\ 1 + \sqrt{i} & i = j. \end{cases}$$

In all our experiments, the right-hand side vectors are generated randomly with coefficients in $[0, 1]$ while the tolerance for the stopping criteria is set equal to 10^{-5} .

Note that matrices with different degree of decay are equally difficult for the standard Cholesky based solver. In contrast, for iterative solvers, such as the CG based method, matrices that exhibit strong decay (i.e., high d) are easier to solve with respect to those with a small or null decay, since they become strongly diagonally dominant.

(a) Time and energy analysis

Figure 9 illustrates time-to-solution and energy consumption to solve problem (3.1) or (3.2) with different iterative refinement based methods and for a range of complete and approximate covariance matrices, with $d = [1, 2, 4]$. All the quantities are calculated without accounting for the initialization phase. The Cholesky based method shows no difference with respect to the degree of decay, since it has a fixed complexity that depends only on the matrix size. A similar result is also obtained for the non-banded CG based method. However, by using the banded CG version we observe a sensible progressive reduction in the time-to-solution, and thus in the total consumed energy.

To quantify the benefits of the banded CG based method with respect to the other approaches, in Table 2 we report the values obtained for a covariance matrix with $n = 70000$. In most of the cases, the banded CG based version is able to reduce the time-to-solution by a factor ten or more, with respect to the non-banded version. This gain is mainly due to the reduced time cost of each low precision iteration. This is evident in the case $d = 4$, where the banded CG based version converges between 15 and 30 times faster

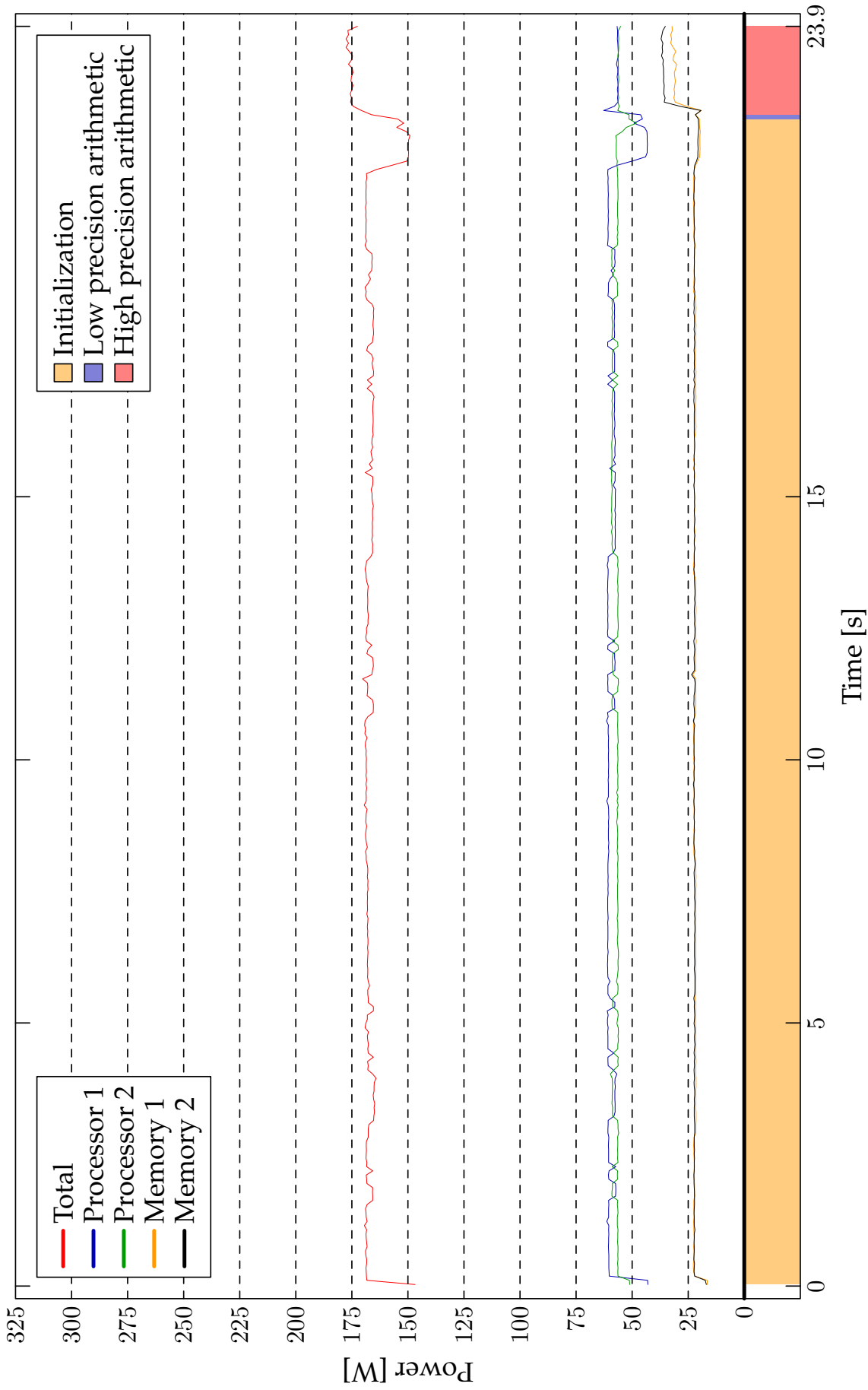


Figure 7: Power diagrams on IBM PS702 Blade Server during the solution of a dense linear system with 1 right-hand side using the banded conjugate gradient algorithm with iterative refinement. In the timeline, each computational phase is displayed with a different color.

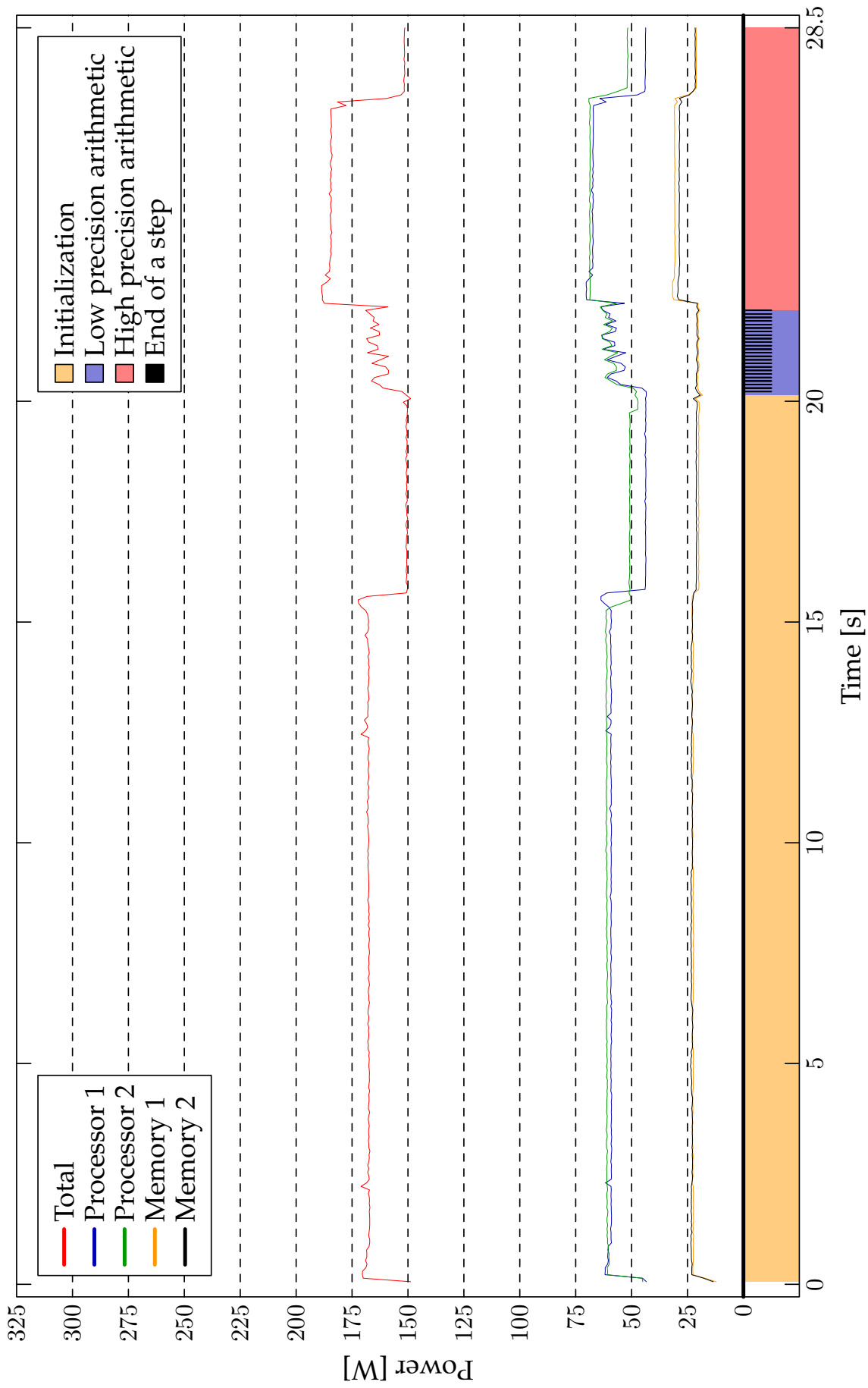
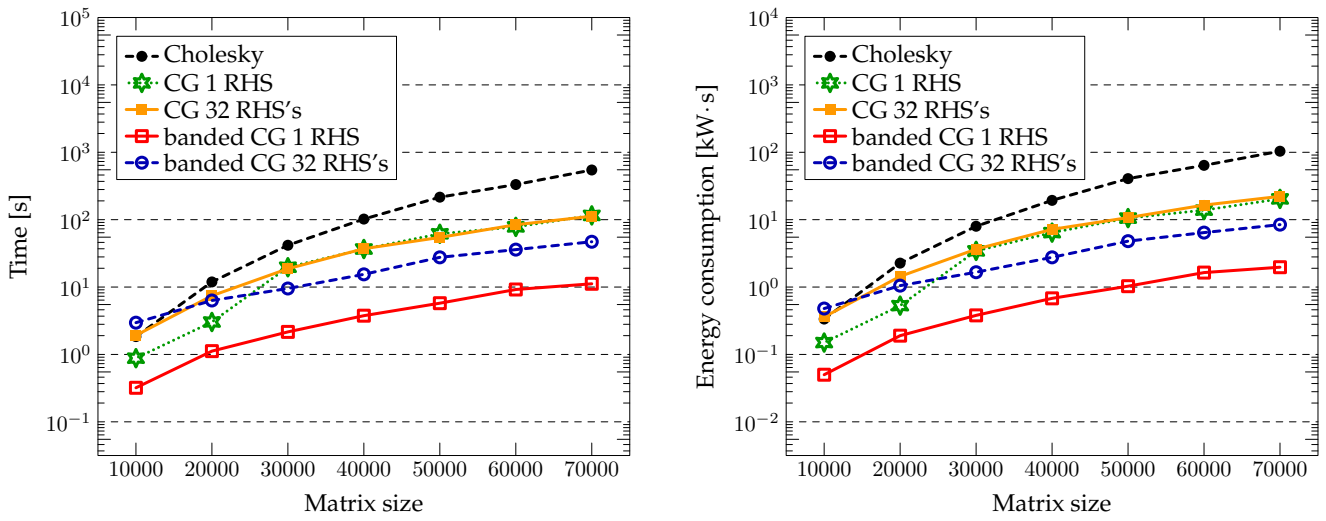
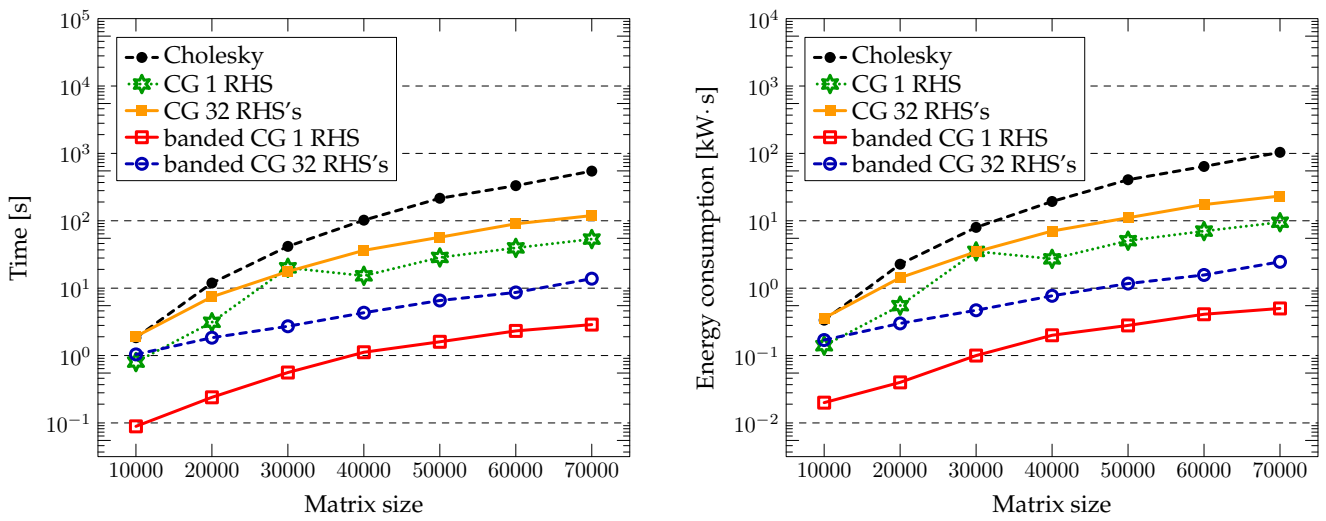


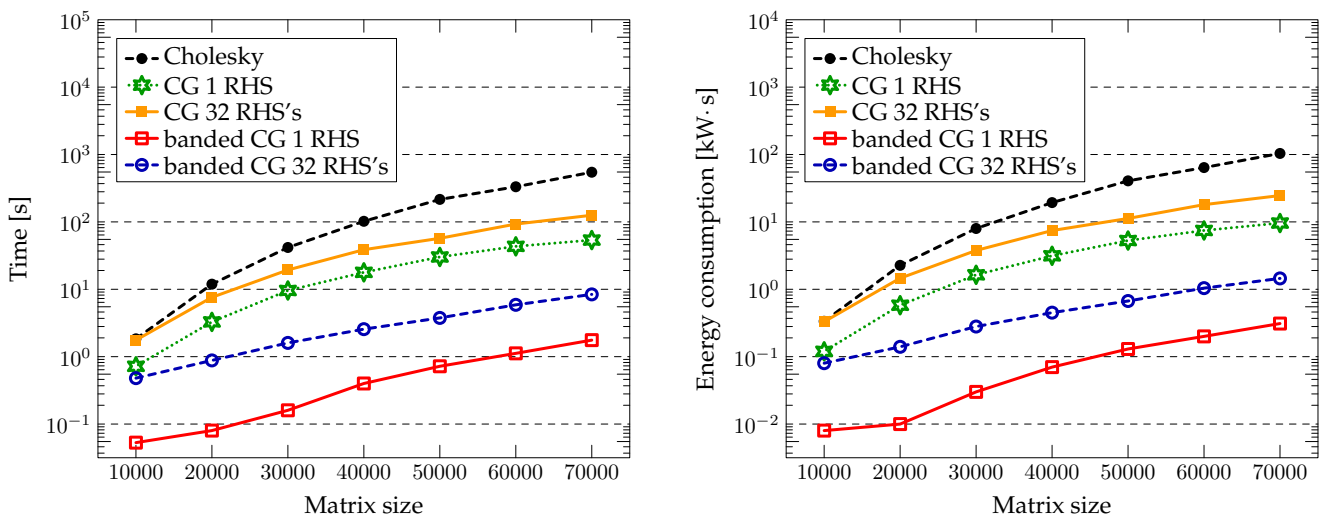
Figure 8: Same as Figure 7 but for 32 right-hand sides. In the timeline, each computational phase is displayed with a different color, while the end of each step is marked by a black line.



(a)



(b)



(c)

Figure 9: Time and energy comparison between different methods for the solution of power model covariance matrices of different size. (a) $d = 1$. (b) $d = 2$. (c) $d = 4$.

Table 2: Comparison of different methods to solve a model covariance matrix, with $n = 70000$.

	RHS's	Iterations [low/high]	Time [s]	Average power [W]	Standard error [W]	Energy [kW·s]	TOP500 [GFlops]	Green500 [GFlops/W]
<i>d = 1</i>								
Cholesky	32	1 / 1	546.0	190.0	13.5	103.7	214.4	1.11
CG	1	179 / 2	115.7	175.7	3.2	20.3	15.3	0.09
CG	32	83 / 1	112.5	197.1	7.5	22.2	233.8	1.19
Banded CG	1	691 / 8	11.2	175.9	6.2	2.0	7.1	0.04
Banded CG	32	692 / 8	47.0	179.4	15.3	8.4	54.3	0.30
<i>d = 2</i>								
Cholesky	32	1 / 1	546.0	190.0	13.5	103.7	214.4	1.11
CG	1	83 / 1	53.5	177.8	3.1	9.5	15.3	0.09
CG	32	85 / 1	119.3	195.2	11.2	23.3	225.9	1.16
Banded CG	1	173 / 2	2.9	174.4	7.0	0.5	6.3	0.04
Banded CG	32	177 / 2	13.8	177.6	14.6	2.5	46.1	0.26
<i>d = 4</i>								
Cholesky	32	1 / 1	546.0	190.0	13.5	103.7	214.4	1.11
CG	1	85 / 1	53.8	179.0	1.8	9.6	15.7	0.09
CG	32	88 / 1	125.5	195.0	10.8	24.6	222.2	1.13
Banded CG	1	85 / 1	1.8	174.1	4.9	0.3	5.5	0.03
Banded CG	32	88 / 1	8.4	172.6	14.2	1.5	37.8	0.22

than the non-banded version, despite the number of low and high precision iterations is exactly the same for both methods. In addition the peak power consumption does not increase when solving for more than one right-hand side, leading to an additional reduction in the total energy consumed by the problem. For instance, in the case of $d = 4$ and $n = 70000$, the energy consumed by the banded CG version with 32 right-hand sides is just 6% of the energy consumed by the non-banded CG version to solve exactly the same problem.

(b) Standard performance metrics analysis

Despite the energy analysis in the previous section highlighted the strong potential of the inexact iterative refinement strategy, by ranking the methods with standard metrics, i.e., the TOP500 [GFlops] and the Green500 [GFlops/W], we obtain a surprising result: the banded CG based method scores quite poorly in both rankings (see Table 2, rightmost columns).

This behavior is also confirmed in Figure 10, for a large range of matrix sizes. The motivations behind these results are linked to the nature of the employed methods. On the one hand, the Cholesky and the non-banded CG (especially with multiple right-hand

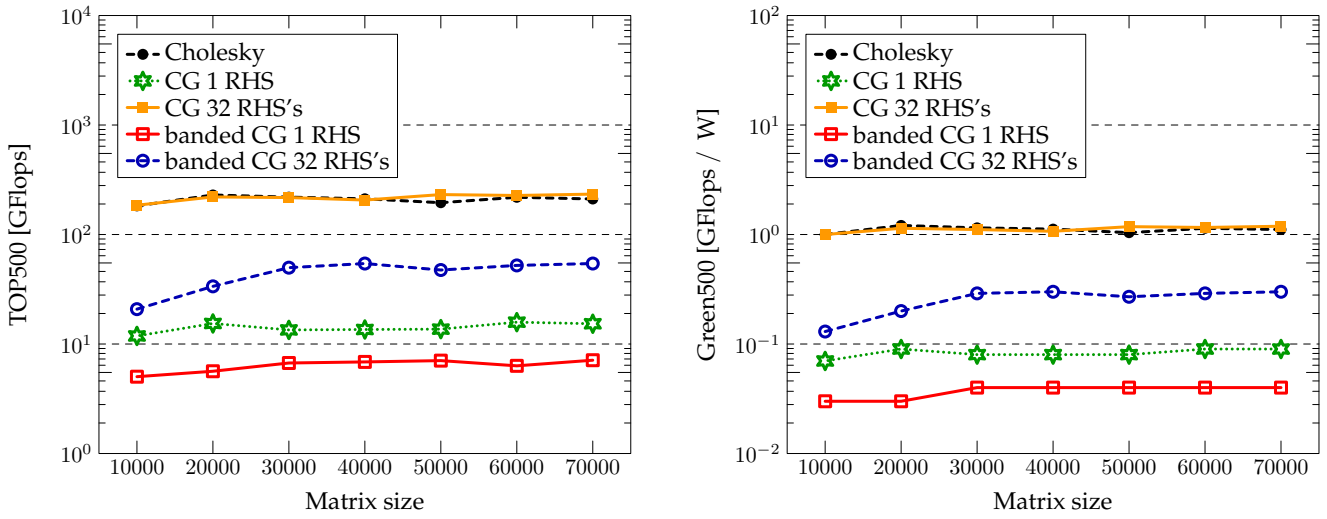
sides) based methods make extensive use of computational resources, performing a very large number of operations per second to factorize the matrix and to perform dense matrix-vector multiplications, respectively. On the other hand, the banded CG based method performs much less multiplications per second, due to the reduced effective size of the matrix, which is also stored in a different format. Therefore, the number of BLAS-2 and BLAS-3 operations for the banded CG based method is drastically reduced, leading to a poor score in the TOP500 ranking.

Regarding energy, we observe that the curves in the right graphs are quite similar to those for the time on the left. The reason is that average power differs for methods by at most 20 W, so that it has a very low impact on the energy trend with respect to time-to-solution, which is dominant. This also reflects in the Green500 ranking, where the result is dominated by the number of GFlops, regardless of the effective average power consumption, and thus leading to similar conclusions with respect to the TOP500 ranking. However, those 20 W actually corresponds to a significant 33% difference with respect to the net power consumption (from 142.1 W up to 200 W).

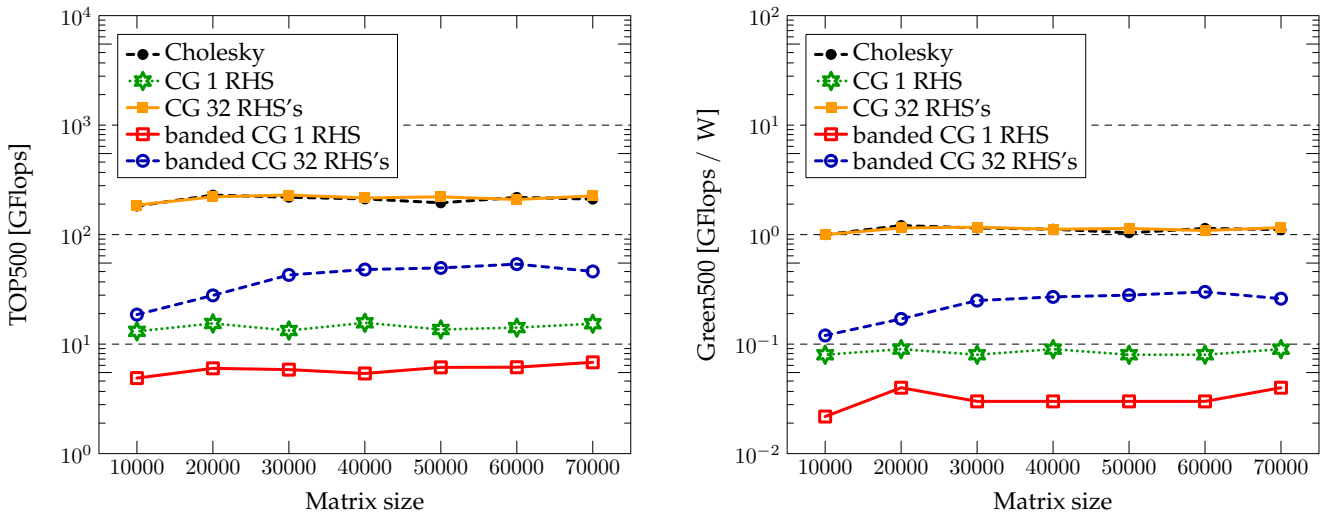
In summary, our results show clearly that standard metrics are not able to capture the real behavior of applications, and this is mainly due to the fact that they rank methods and machines on the base of GFlops and GFlops/W rather than real quantities of practical interest, i.e., time-to-solution and energy. In this regard, the new strategies proposed in [2] represent a first step towards the development of concrete energy-aware metrics which, combined with the use of methods as CG in place of LINPACK, can drive the development of future hardware in the correct direction.

5. Conclusions

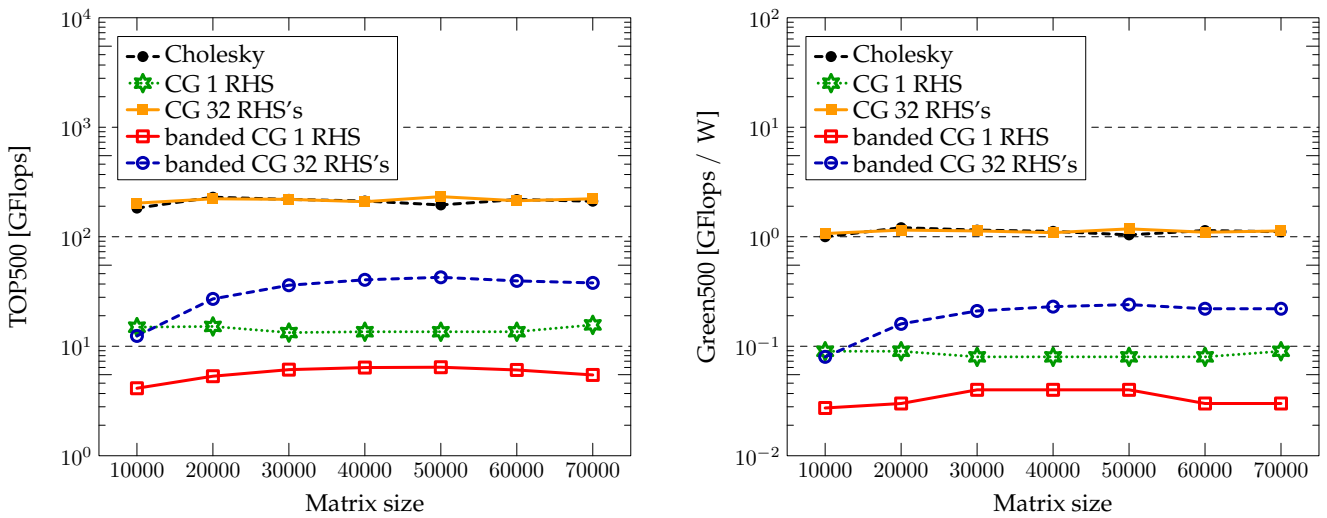
Power awareness and energy consumption is quickly becoming a central issue in HPC systems and research. There is rich recent activity towards solutions that allow us to continue historical exponential improvements in performance while at the same time keeping power requirements at affordable levels. Towards this direction, we described here our recent advancements in the context of energy-aware performance metrics for HPC systems. More in detail, we developed a framework for accurate, on chip and on-line power measurements, with minimal distortion of user runs. Our tool allows the easy instrumentation of user code which subsequently enables its detailed power profiling. We demonstrated the validity and superiority of our proposed performance metrics on actual energy measurements. Finally, we described a framework that combines different precision levels and relaxes data fidelity, and thus has the potential to reduce energy by a few orders of magnitude.



(a)



(b)



(c)

Figure 10: Standard metrics applied to a range of methods for the solution of power model covariance matrices of different size. (a) $d = 1$. (b) $d = 2$. (c) $d = 4$.

Acknowledgments

This work was completed during an internship of the first author at the Computational Sciences Group, IBM Research - Zurich. The first author is also partially supported by CE-ITI (P202/12/G061 of GAČR).

The project Exa2Green (under grant agreement n°318793) acknowledges the financial support of the Future and Emerging Technologies (FET) programme within the ICT theme of the Seventh Framework Programme for Research (FP7/2007-2013) of the European Commission. IBM, ibm.com, ESSL, and POWER7 are trademarks or registered trademarks of International Business Machines Corp., registered in many jurisdictions worldwide. Other product and service names might be trademarks of IBM or other companies. A current list of IBM trademarks is available on the Web at “Copyright and trademark information” at: www.ibm.com/legal/copytrade.shtml.

References

1. K. Asanovic, R. Bodik, B. C. Catanzaro, J. J. Gebis, P. Husbands, K. Keutzer, D. A. Patterson, W. L. Plishker, J. Shalf, S. W. Williams, and K. A. Yelick.
The landscape of parallel computing research: a view from Berkeley.
Technical Report UCB/EECS-2006-183, University of California, Berkeley, December 2006.
2. C. Bekas and A. Curioni.
A new energy aware performance metric.
Computer Science - Research and Development, 25(3–4):187–195, 2010.
3. C. Bekas and A. Curioni.
Processing of linear systems of equations, 2012.
US Patent, US 2012/0005247 A1.
4. C. Bekas, A. Curioni, and I. Fedulova.
Low-cost data uncertainty quantification.
Concurrency and Computation: Practice and Experience, 24(8):908–920, 2012.
5. L. Brochard, R. Panda, and S. Vemuganti.
Optimizing performance and energy of HPC applications on POWER7.
Computer Science - Research and Development, 25(3–4):135–140, 2010.
6. J. J. Dongarra, P. Luszczek, , and A. Petitet.
The LINPACK benchmark: past, present, and future.
Concurrency and Computation: Practice and Experience, 15(9):803–820, 2003.
7. M. Floyd, B. Brock, M. Allen-Ware, K. Rajamani, B. Brock, C. Lefurgy, A. J. Drake, L. Pesantez, T. Gloekler, J. A. Tierno, P. Bose, and A. Buyuktosunoglu.
Introducing the adaptive energy management features of the POWER7 chip.
IEEE Micro, 31(2):16 pages, 2011.
8. R. Ge, X. Feng, S. Song, H.-C. Chang, D. Li, and K. W. Cameron.
PowerPack: energy profiling and analysis of high-performance systems and applications.
IEEE Transactions on Parallel and Distributed Systems, 21(5):658–671, 2009.
9. G. H. Golub and C. F. Van Loan.
Matrix Computations.

- The Johns Hopkins University Press, Baltimore, 1996.
10. N. Halko, P. G. Martinsson, and J. A. Tropp.
Finding structure with randomness: probabilistic algorithms for constructing approximate matrix decompositions.
SIAM Review, 53(2):217–288, 2011.
 11. N. J. Higham.
Accuracy and Stability of Numerical Algorithms.
SIAM, Philadelphia, 1996.
 12. E. L. Kaltofen.
The “seven dwarfs” of symbolic computation.
In *Numerical and Symbolic Scientific Computing*, pages 95–104. Springer, 2012.
 13. J. O. Kephart, H. Chan, R. Das, D. W. Levine, G. Tesauro, F. Rawson, and C. Lefurgy.
Coordinating multiple autonomic managers to achieve specified power-performance tradeoffs.
In *Proceedings of the 4th IEEE Conference on Autonomic Computing (ICAC’07)*, Jacksonville, Florida, USA, June, 11–15 2007.
 14. M. Knobloch, M. Foszczynski, W. Homberg, D. Pleiter, and H. Böttiger.
Mapping fine-grained power measurements to HPC application runtime characteristics on IBM POWER7.
Computer Science - Research and Development, pages 1–9, 2013.
 15. P. Kogge.
The road to exascale: hardware and software challenges panel.
In *SC09: Exa Panel.*, Portland, Oregon, USA, November, 14–19 2009.
 16. C. Lefurgy, X. Wang, , and M. Ware.
Server-level power control.
In *Proceedings of the 4th IEEE Conference on Autonomic Computing (ICAC’07)*, Jacksonville, Florida, USA, June, 11–15 2007.
 17. D. Watts, K. Anders, and B. Patel.
IBM BladeCenter PS700, PS701, and PS702 technical overview and introduction.
Technical Report REDP-4655-00, IBM, July 2012.

About Philosophical Transactions of the Royal Society A

Information copied from the website <http://rsta.royalsocietypublishing.org>.

Each issue of *Philosophical Transactions A* is devoted to a specific area of the mathematical, physical and engineering sciences. This area will define a research frontier that is advancing rapidly, often bridging traditional disciplines.

All articles are peer reviewed and edited to the highest standards. We currently publish 24 issues per year and, along with all Royal Society journals, we are committed to archiving and providing perpetual access.

The Royal Society was founded in 1660 to promote the new experimental philosophy of that time, embodying the principles of Sir Francis Bacon. Henry Oldenburg was appointed as the first (joint) secretary to the Society and he was also the first editor of the Society's journal *Philosophical Transactions*. The first issue of *Philosophical Transactions* appeared in March 1665 and featured Oldenburg's correspondence with leading European scientists. In its formative years Isaac Newton had seventeen papers published in the journal including his first paper – *New Theory about Light and Colours* – which effectively served to launch his scientific career in 1672. In the same year his new reflecting telescope was described and the original drawing was also published in the journal. *Philosophical Transactions* has also published the work of Charles Darwin, Michael Faraday, William Herschel and many more celebrated names in science.

In 1887 the journal expanded to become two separate publications, one serving the biological sciences and the other serving the physical sciences.

Philosophical Transactions of the Royal Society has the prestige of being the world's first scientific journal.

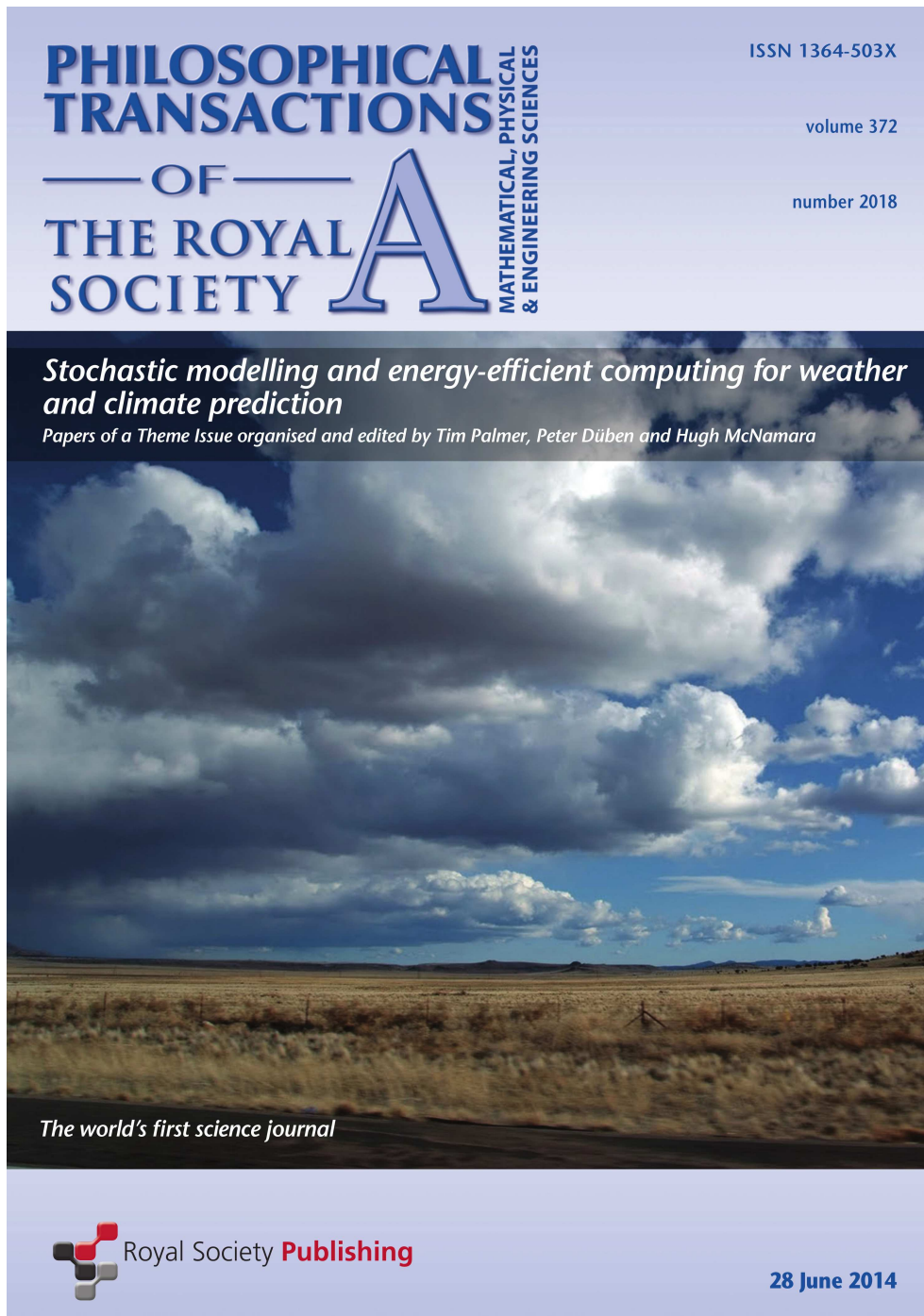


Figure 11: The cover of Philosophical Transactions of the Royal Society A: Physical, Mathematical and Engineering Sciences 372(2018), 2014, the Theme Issue 'Stochastic modelling and energy-efficient computing for weather and climate prediction'.